⌘ *Author's Choice*

Identification of a Mammalian-type Phosphatidylglycerophosphate Phosphatase in the Eubacterium *Rhodopirellula baltica**

Phildrich G. Teh[‡], **Mark J. Chen**[§¶], **James L. Engel**[‖], **Carolyn A. Worby**[‖], **Gerard Manning**[§¶], **Jack E. Dixon**[‡‖**‡‡1], and **Ji Zhang**[‖2]

From the Departments of [‡]*Chemistry and Biochemistry,* [‖]*Pharmacology, and* **Cellular and Molecular Medicine, University of California San Diego, La Jolla, California 92093, the* [§]*Razavi Newman Center for Bioinformatics, Salk Institute for Biological Studies, La Jolla, California 92037, the* [¶]*Department of Bioinformatics and Computational Biology, Genentech, South San Francisco, California 94080, and the* [‡‡]*Howard Hughes Medical Institute, Chevy Chase, Maryland 20815*

Background: PTPMT1 is the mitochondrial phosphatidylglycerophosphate (PGP) phosphatase essential for the biosynthesis of cardiolipin, an integral component of mitochondrial and bacterial membranes.
Results: A PTPMT1-like phosphatase in the bacterium *Rhodopirellula baltica* has similar PGP phosphatase activity as its mammalian ortholog.
Conclusion: PTPMT1 is evolutionarily conserved.
Significance: The existence of a mammalian-type PGP phosphatase in bacteria provides new insight into the evolution of cardiolipin metabolism.

Cardiolipin is a glycerophospholipid found predominantly in the mitochondrial membranes of eukaryotes and in bacterial membranes. Cardiolipin interacts with protein complexes and plays pivotal roles in cellular energy metabolism, membrane dynamics, and stress responses. We recently identified the mitochondrial phosphatase, PTPMT1, as the enzyme that converts phosphatidylglycerolphosphate (PGP) to phosphatidylglycerol, a critical step in the *de novo* biosynthesis of cardiolipin. Upon examination of PTPMT1 evolutionary distribution, we found a PTPMT1-like phosphatase in the bacterium *Rhodopirellula baltica*. The purified recombinant enzyme dephosphorylated PGP *in vitro*. Moreover, its expression restored cardiolipin deficiency and reversed growth impairment in a *Saccharomyces cerevisiae* mutant lacking the yeast PGP phosphatase, suggesting that it is a *bona fide* PTPMT1 ortholog. When ectopically expressed, this bacterial PGP phosphatase was localized in the mitochondria of yeast and mammalian cells. Together, our results demonstrate the conservation of function between bacterial and mammalian PTPMT1 orthologs.

Reversible phosphorylation, a dynamic process carried out by kinases and phosphatases, is vital for the regulation of many cellular signaling events (1, 2). More than 100 human genes encode proteins of the same fold as the classic protein tyrosine phosphatases (PTPs)[3] and feature the highly conserved Cys-X_5-Arg (CX_5R) motif in their active site. These phosphatases were once thought to exclusively dephosphorylate phosphotyrosine. More recent studies, however, have identified several PTPs that can hydrolyze phosphate from phosphoserine/threonine-containing proteins or even nonprotein substrates (3, 4). For instance, the tumor suppressor PTEN and the carbohydrate binding Laforin have been shown to dephosphorylate phosphoinositides and glycogen respectively, both *in vitro* and *in vivo* (5–7). The primary amino acid sequences of these phosphatases vary from the classical tyrosine-specific PTPs; therefore, they are categorized into a subfamily called dual specificity phosphatases (DSPs) (2).

We recently characterized a new DSP called PTPMT1 (PTP localized to the mitochondrion 1). Interest in this protein arose due to its strong active site similarity to PTEN. PTPMT1 is the first PTP localized exclusively to the mitochondrion; specifically, it resides in the inner membrane facing the matrix (8). Our recent results identify PTPMT1 as the mammalian phosphatase that mediates the conversion of phosphatidylglycerophosphate (PGP) into phosphatidylglycerol (PG), a step necessary for the *de novo* biosynthesis of cardiolipin (CL) (Fig. 1A) (9).

CL is an anionic phospholipid found in most bacteria and eukaryotes[4] (10). It is an essential component of the inner mitochondrial membrane in eukaryotes and regulates mitochondrial ATP production, protein import, and apoptosis (10). In bacteria, CL is one of the major anionic phospholipids and functionally interacts with membrane proteins that are involved in energy metabolism and cellular division (11).

[1] To whom correspondence may be addressed: Department of Pharmacology, University of California San Diego, CA. Tel.: 858-822-0684; Fax: 858-822-5888; E-mail: jedixon@ucsd.edu.
[2] To whom correspondence may be addressed: Department of Pharmacology, University of California San Diego, CA. Tel.: 858-822-0684; Fax: 858-822-5888; E-mail: jz3@ucsd.edu.

[3] The abbreviations used are: PTP, protein tyrosine phosphatase; DSP, dual specificity phosphatase; PTPMT1, PTP localized to mitochondrion 1; PGP, phosphatidylglycerophosphate; PG, phosphatidylglycerol; CL, cardiolipin.
[4] Cardiolipin analogues are found in Archaea but contain unique diphytanylglycerol diether lipid, in contrast to the largely diacylglycerol-derived membrane lipids in eukaryotes and bacteria (48).

Eukaryotes and bacteria utilize a similar strategy to synthesize CL, except in the step of producing CL from PG (12). Therefore, we thought it would be interesting to search for a PTPMT1-like phosphatase in bacteria.

In this study, we have characterized a putative PTPMT1 ortholog in the bacterium *Rhodopirellula baltica*. We show that this protein functions as a PGP phosphatase and is localized to the mitochondrion when ectopically expressed in yeast or mammalian cells, suggesting that the function of PTPMT1 is evolutionarily conserved. Together, our results contribute to the understanding of the evolution of CL metabolism.

EXPERIMENTAL PROCEDURES

Sequences and Phylogenetic Analysis—Bacterial PTPMT1-like sequences were first collected by searching human PTPMT1 against NCBI non-redundant (NR) database and were then inspected for containing conserved motifs found in eukaryotic PTPMT1s. The phylogenetic tree of selected human and bacterial DSPs was built using only the phosphatase domains. Sequences were aligned by PROMALS3D (13) and adjusted manually. Phylogenetic trees were inferred by using maximum likelihood (ML) and neighbor joining (NJ) methods in MEGA 5.0 (14). Different models of Poisson Correction, Dayhoff matrix, Jones-Taylor-Thornton (JTT) matrix, and JTT + frequency (F) were used, and they are consistent with each other on reliable branches. Support for each interior branch was tested with 100 and 1,000 bootstrap replicates for ML and NJ analyses, respectively. The domain structures of PGP phosphatases were analyzed using PFAM, CDD, and PROSITE (15–17).

Protein Expression and Purification—*Mus musculus, Drosophila melanogaster*, and *R. baltica* PTPMT1 orthologs were expressed as fusion proteins with N-terminal GST tag in *Escherichia coli* BL21 (DE3) CodonPlus RIPL cells (Stratagene) (18). The expression plasmids were constructed by ligating the PCR products of PTPMT1 orthologs into the vector. Cultures were grown at 37 °C in LB medium containing chloramphenicol (34 μg/ml) and kanamycin (50 μg/ml) to an A_{600} of 0.6. Cultures were then induced with isopropyl-1-thio-β-D-galactose pyranoside (IPTG) to a final concentration of 0.4 mM and allowed to grow overnight at 25 °C. Cells were pelleted down, resuspended in 25 mM Tris, pH 8.0, 150 mM NaCl, 1 mM EDTA, 10% glycerol, 0.5 mM TCEP [Tris(2-carboxyethyl)phosphine], 1 mM Pefabloc SC, 1 mM bezamidine-HCl, 1 mM PMSF (phenylmethylsulphonyl fluoride), and lysed using a high pressure homogenizer (Avestatin EmulsiFlex C5). Next, the lysed samples were centrifuged at 19,000 rpm for 30 min to remove insoluble material. The resulting supernatants were purified by affinity chromatography using GST-bind resin (Novagen). Finally, fusion proteins were eluted with 50 mM Tris, pH 8.0, 150 mM NaCl, 1 mM EDTA, 10% glycerol, and 15 mM reduced glutathione. Catalytically inactive mutants (CS) were generated using site-directed mutagenesis and similarly purified.

Phosphatase Assays—Phosphatase assays using para-nitrophenylphosphate (pNPP) or [^{14}C]PGP were carried out in assay buffer containing 50 mM sodium acetate, 25 mM bis-Tris, 25 mM Tris, and 2 mM dithiothreitol. The pH of the assay buffer was set at 5.5 for *M. musculus* PTPMT1, 7.0 for *D. melanogaster*, and 8.5 for *R. baltica* protein. pNPP assays were carried out at 37 °C for 10 min as previously described (19). For PGP assays, the ^{14}C-labeled PGP was synthesized as previously described (20). Briefly, the reaction was carried out in the presence of 0.1 M Tris-HCl, pH 8.0, 0.1% Triton X-100, 0.2 mM CDP-DAG (Avanti Polar Lipids), 0.5 mM glycerol-3-phosphate (Sigma), and 13 μM sn-[U-^{14}C]glycerol-3-phosphate (2–4 μCi/μmol, American Radiolabeled Chemicals). The reaction was initiated by the addition of recombinant *E. coli* PGP synthase and 0.1 M MgCl$_2$ (18). After incubation at 37 °C for 2 h, 0.5 ml of 0.1 N HCl in methanol, 1.5 ml of chloroform, and 3.0 ml of 1 M MgCl$_2$ were added to stop the reaction. The organic phase was then extracted and dried under vacuum. The resulting ^{14}C-PGP was resuspended in 10 mM Tris pH 7.4 via sonication for 5 min. 1.25×10^4 cpm of this radiolabeled PGP and 2 μg of recombinant enzymes were then added to the assay buffer. Reactions were incubated at 37 °C for 10 min and quenched by the addition of 0.5 ml of 0.1 N HCl in methanol, 1.5 ml of chloroform, and 3.0 ml of 1 M MgCl$_2$. After extraction, the resulting lipid products were resuspended in chloroform. A Whatman silica gel 60 plate was activated by baking for 1 h at 180 ^{0}F under vacuum conditions. The TLC plate was then spotted with the resuspended lipids, dried for 10 min in a fume hood, and developed in a chamber containing chlorofom/methanol/glacial acetic acid (65:25:8). The plate was exposed to a storage phosphor screen and analyzed using a Typhoon 9410 phosphorimager (GE Healthcare).

A malachite green assay was used to quantitatively measure the phosphatase activity (21). The enzyme reactions were carried out in 20 μl of 50 mM sodium acetate, 25 mM bis-Tris, 25 mM Tris, 2 mM dithiothreitol, and indicated amounts of PGP. The pH of assay buffer for each enzyme was described above. Reactions were initiated by the addition of enzyme followed by incubation at 30 °C. Reactions were subsequently terminated by the addition of 20 μl of 0.1 M *N*-ethylmaleimide and spun down to sediment the lipid aggregates. Twenty-five microliters of the supernatant was added to 50 μl of malachite green reagents and vortexed. Absorbance was measured at 620 nm. The recombinant proteins were free of inorganic phosphate. The nonenzymatic hydrolysis of the substrate was corrected by measuring the increase in the absorbance without the addition of the enzymes.

^{32}P-labeling of Yeast Cells and Lipid Extraction—The plasmids for complementation assays were assembled by inserting the PCR products of the PTPMT1 orthologs with a C-terminal FLAG tag into the pRS415-GPD vector (ATCC). *GEP4* knockout yeast strains are derivatives of S288C obtained from Open-Biosystems (22). After verification by gene-specific PCR, *gep4∆* cells were transformed with PTPMT1-encoding plasmids. Cells were grown in YPD at 30 °C until mid-log phase followed by the addition of radiolabeled ^{32}P to the concentration of 10 μCi/ml for 12 h. Lipids were isolated as previously described (23). Briefly, cells were resuspended in solution containing 0.5 M NaCl in 0.1 N HCl and vortexed with glass beads. Lipids were extracted, dried under vacuum, and separated via TLC. For visualizing cardiolipin, a Whatman silical gel 60 plate was used and prepared as described above. The separating solution used was chloroform/methanol/ammonium hydroxide/water (130:

75:2:6). For visualizing PGP, a HPTLC silica gel 60 plate was used and the separating solution used was ethyl acetate/isopropanol/ethanol/ammonium hydroxide/water (12:36:12:7.2:28.8) (24). Individual species were identified by co-migration of non-radiolabeled standards. The relative abundance of PGP and CL were determined by using the Typhoon 9410 Variable Mode Imager and ImageQuant TL software, and were statistically analyzed using a Student's *t* test.

Yeast Complementation Assay—The *gep4Δ* cells were transformed and grown at 30 °C to mid-log phase as described above. Cells were counted and serially diluted 5-fold. Each dilution was spotted onto either YPD plates or Synthetic Completed Medium with Dextrose (SCD) in the presence of 25 μg/ml ethidium bromide. Plates were incubated for 2 days at the indicated temperatures. For Western blot analysis, 5 A_{600} of cells were pelleted. Proteins were precipitated with 50% trichloroacetic acid and resuspended in SDS/PAGE loading buffer. Monoclonal anti-Flag antibody was used for analysis (Sigma).

Mitochondrial Fractionation—500 ml cultures of *gep4Δ* cells transformed with plasmids encoding either the *D. melanogaster* or *R. baltica* PTPMT1 were grown in YPD at 30 °C to A_{600} of 2. The purified mitochondria were isolated as previously described (25). Briefly, cells were resuspended in sorbitol buffer, converted to spheroblasts by zymolase treatment, and homogenized. Crude mitochondria were isolated via a low-speed centrifugation (1,500 $\times$ *g*) followed by a high-speed spin (12,000 $\times$ *g*). Further purification was achieved by histodenz gradient centrifugation.

Immunofluorescence Analysis—The plasmid for the immunofluorescence assay was constructed by ligating the PCR product of *R. baltica* PTPMT1 into the pEGFP-N1 vector. The plasmid was transfected into COS1 cells using Fugene 6 (Roche). MitoTracker Red was added to cells in DMEM to a concentration of 100 n$_M$ and incubated at 37 °C for 30 min before fixation with 4% paraformaldehyde and permeabilization with ice-cold acetone.

RESULTS

Identification of a Putative PTPMT1 Ortholog in R. baltica—PTPMT1 is a member of the DSP family and its putative orthologs have been identified in many species of mammals, plants, protists, and even bacteria (26). Among the bacterial sequences identified by searching the NCBI database, the *R. baltica* and *Blastopirellula marina* proteins display the closest homology to the *Homo sapiens* PTPMT1, with 48 and 46% sequence similarity, respectively (Fig. 1*B*). They also contain other PTPMT1-like features such as a predicted transmembrane domain, an active site CX_5R motif with basic residues, and a WPD loop shown to be important for the formation of the thiophosphoryl intermediate and its subsequent hydrolysis (Fig. 1*B*) (18). Notably, *Rhodopirellula* and *Blastopirellula* belong to the bacterial phylum *Planctomycetes* and contain many unique eukaryote-like features, such as intracellular compartmentalization (27, 28). Some studies have suggested that planctomycetes might be an evolutionary intermediate in the transition from prokaryotes to eukaryotes (29). Because of the conserved requirement for CL in both bacteria and eukaryotes,

it is of interest to determine whether PTPMT1 orthologs in planctomyocytes are functional PGP phosphatases.

To obtain insight into the sequence homology of PTPMT1-like phosphatases, we built a phylogenetic tree of human DSPs (Fig. 1*C*). *Homo sapiens* PTPMT1 clustered distantly from phosphatases that are known to dephosphorylate proteins, such as the MAP kinase phosphatases (MKP) (30). Interestingly, *Rhodopirellula* and *Blastopirellula* PTPMT1 orthologs grouped relatively close to human PTPMT1. However, because the phylogenetic tree does not guarantee orthology or functional homology, we sought to characterize the enzymatic activity of the PTPMT1-like phosphatase in bacteria.

The Rhodopirellula PTPMT1 Dephosphorylates PGP in Vitro—To test the functional conservation of PTPMT1 from diverse species, we compared the phosphatase activities of the *R. baltica*, *D. melanogaster*, and *M. musculus* orthologs. Each gene was cloned into bacterial expression vectors, expressed, and affinity purified. The pH/rate profiles of these recombinant proteins against the artificial phosphotyrosine analog pNPP were obtained. The catalytic activities of *M. musculus*, *D. melanogaster*, and *R. baltica* PTPMT1 variants were most efficient at pH 5.5, 7.0, and 8.5, respectively (data not shown). Subsequently, the specific activities of all orthologs were measured at their respective optimum pH using pNPP as the substrate (Fig. 2*A*). Although the *M. musculus* and *D. melanogaster* PTPMT1s were more active, the bacterial variant still possessed measurable phosphatase activity against pNPP. As expected, active site cysteine to serine mutants (CS) were catalytically inactive. The specific activity of PTPMT1 orthologs against pNPP was relatively low compared with other PTPs that dephosphorylate proteins, such as dPTP61F and VHR (19). However, the inability to efficiently dephosphorylate pNPP is shared by other lipid phosphatases, like PTEN and myotubularins (19).

We next tested whether these proteins could dephosphorylate PGP, the physiological substrate of mammalian PTPMT1. We enzymatically synthesized radiolabeled PGP by incubating sn-[U-^{14}C]glycerol-3-phosphate with CDP-DAG in the presence of purified recombinant PGP synthase from *E. coli* (Fig. 2*B*) (18, 20). The resulting [^{14}C]PGP was then extracted and incubated with each PTPMT1 ortholog. The reaction components were separated by thin-layer chromatography (TLC) and visualized by autoradiography (Fig. 2*C*). Non-radiolabeled PG standards were observed to migrate toward the middle of the TLC plate, whereas PGP stayed close to the origin (data not shown). Like the *M. musculus* enzyme, *Drosophila*, and *Rhodopirellula* PTPMT1 successfully converted PGP to PG (Fig. 2*C*). Their active site CS mutants along with the glucan phosphatase Laforin, displayed no activity toward PGP.

To further support this finding, we compared the PGP phosphatase activities of *M. musculus*, *D. melanogaster*, and *R. baltica* PTPMT1 orthologs. Determination of enzyme kinetic parameters was hindered by the lack of unlabeled water-soluble substrates. Nonetheless, we examined the activity of each enzyme by measuring the amount of phosphate released in the reaction through a malachite green assay (21). The initial linear rate was first determined by varying enzyme concentration and incubation times (Fig. 2*D*). After establishing the initial rate condition where less than 10% of PGP was dephosphorylated
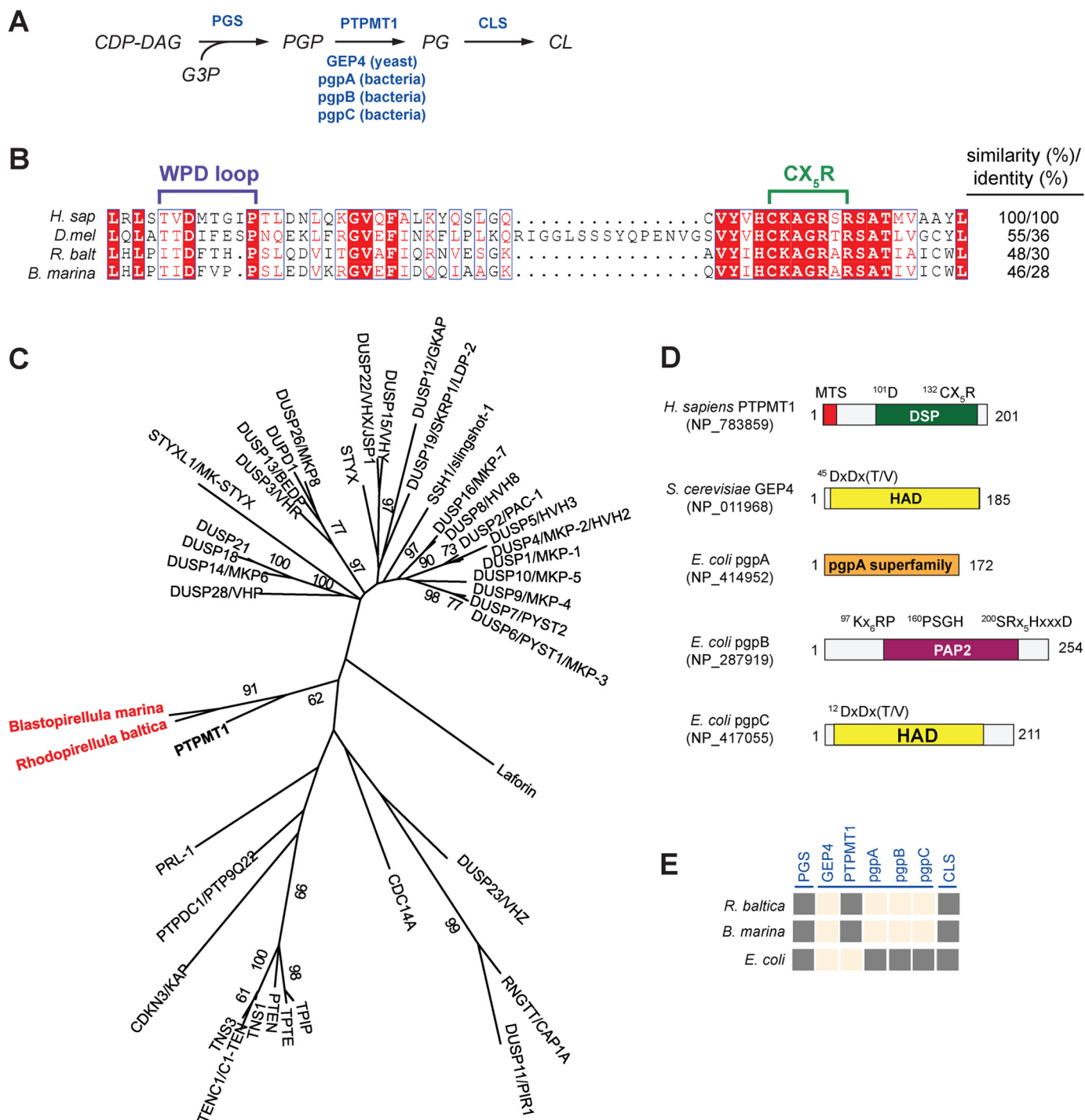
FIGURE 1. **Identification of a putative PTPMT1 ortholog in *R. baltica*.** *A*, schematic diagram of the CL biosynthesis pathway. Enzymes are highlighted in *blue*. CDP-DAG, cytidine diphosphate diacylglycerol; G3P, glycerol-3-phosphate. *B*, active site primary sequence alignment of PTPMT1 orthologs using PROMALS3D and illustrated by ESPript (49, 50). *H. sap* (*H. sapiens*), NP_783859; *D. mel* (*D. melanogaster*), NP_732901; and *R. balt* (*R. baltica*), NP_865112. *C*, a phylogenetic tree of human and bacterial DSPs constructed using maximum likelihood (ML) method in PHYML. Each branch was tested by 100 bootstrap replicates, and only branches with bootstrap values above 50% were shown. Human PTPMT1 is bolded and bacterial PTPMT1 orthologs are highlighted in *red*. *D*, domain architecture of PGP phosphatases. All domains are presented based on analyses using PFAM, CDD, and PROSITE. Catalytic active site sequences are indicated above. *MTS*, mitochondrial targeting sequence; *DSP*, dual specificity phosphatase; *HAD*, haloacid dehalogenase; *PAP2*, phosphatidic acid phosphatase 2. *E*, presence and absence matrix for CL *de novo* synthesis enzymes in *Rhodeopirella*. *Dark gray squares* indicate presence of CL enzyme (column) in target species (row). *Peach squares* mean no ortholog has been identified, *i.e.* blast search failed to identify sequences that meet the bidirectional-best-hit criterion (cut-off E-values of 10^{-10} or less). Sequences of *E. coli* pgsA, *S. cerevisiae* GEP4, *H. sapiens* PTPMT1, *E. coli* pgpA, pgpB, pgpC, and *E. coli* cls1 were used as queries for the blast searches.

during the course of the reaction, we calculated the phosphatase activities of all three enzymes. Compared with *M. musculus* PTPMT1, the *Drosophila* protein was slightly more active,

139% of the mouse enzyme value (Fig. 2*E*). Whereas the *R. baltica* phosphatase contained considerable activity toward PGP, it was less efficient (~50%) than mouse PTPMT1. These results
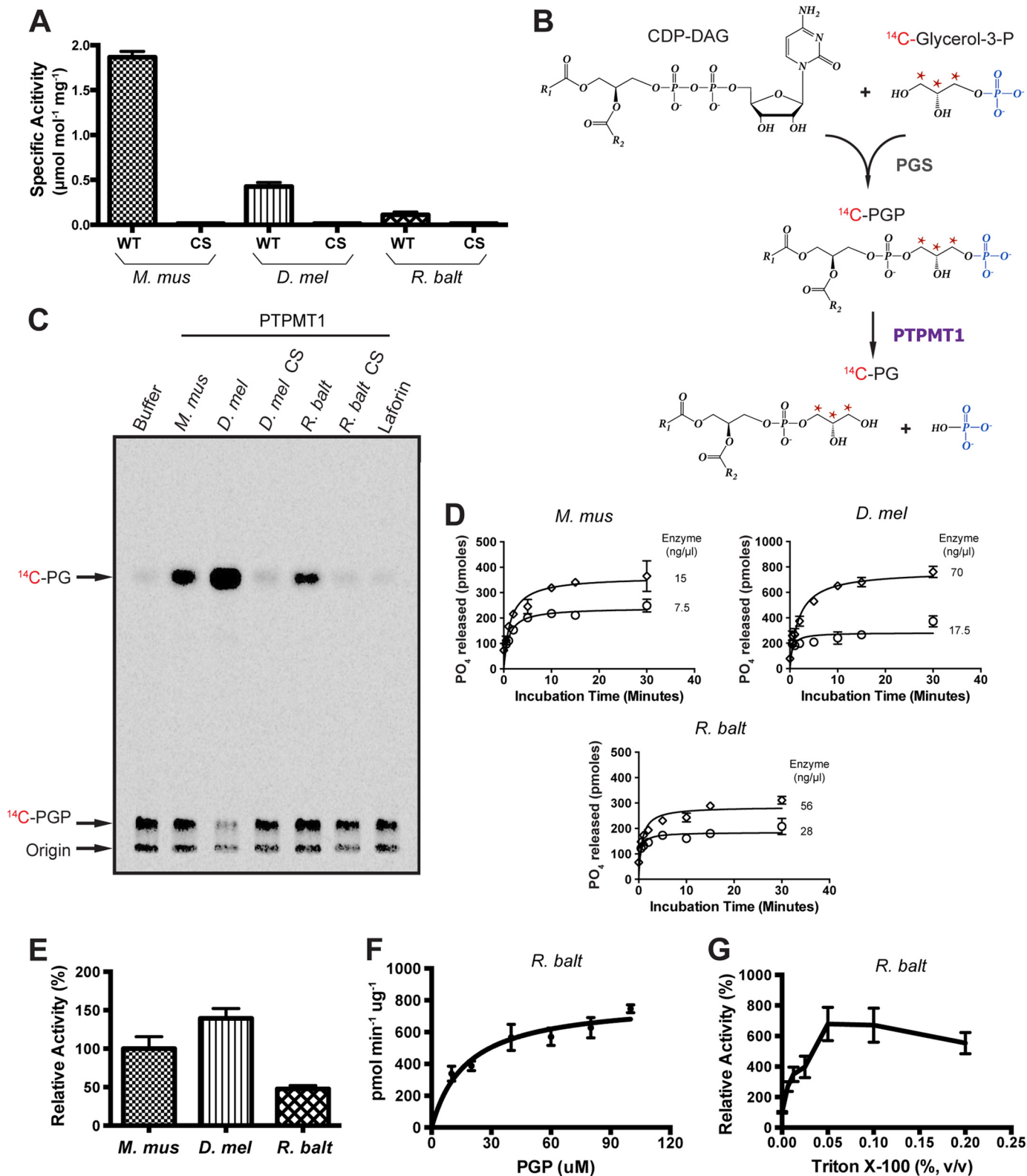
are consistent with the data shown in Fig. 2C, supporting the notion that PTPMT1 orthologs in *Drosophila* and *Rhodopirellula* dephosphorylate PGP *in vitro*.

To further investigate the phosphatase activity of the *Rhodopirellula* PTPMT1 ortholog, we determined saturating substrate levels by incubating the enzyme with various concentrations of PGP. As shown in Fig. 2F, the affinity of *R. baltica* phosphatase for PGP was well below 100 μM, indicating that the PGP concentration utilized in the initial rate determination was not limiting.

Previous studies of *E. coli* and yeast PGP phosphatases have demonstrated that detergents, in particular Triton X-100, sig-

nificantly stimulate their *in vitro* enzymatic activities (31, 32). To examine the effect of Triton X-100 on the *Rhodopirellula* PTPMT1 ortholog, we performed phosphatase assays in the presence of increasing amounts of the detergent. The addition of Triton X-100 substantially increased the PGP phosphatase activity of *Rhodopirellula* PTPMT1 (Fig. 2*G*).

The Rhodopirellula PTPMT1 Functions as a PGP Phosphatase in Vivo—To further validate that the *Rhodopirellula* and *Drosophila* PTPMT1 function as PGP phosphatases, we utilized an *in vivo* yeast complementation system. A PTPMT1 ortholog is not found in fungi (26). However, Osman *et al.* reported that the mitochondrial matrix protein GEP4 possesses PGP phosphatase activity in *Saccharomyces cerevisiae* (24). Deletion of the *GEP4* gene results in an increase of PGP along with a reduction of CL levels. Therefore, we complemented *GEP4*-knock-out yeast with a control plasmid or plasmids encoding either wild type or catalytically inactive forms of PTPMT1 orthologs. The expression of those PTPMT1 orthologs was confirmed by Western blot analysis using anti-FLAG M2 antibody (Fig. 3*A*).

Yeast cells that lack cardiolipin synthase (Crd1p) and PGP synthase (Pgs1p) have respectively been shown to display significant growth deficiency at elevated temperatures or when cultured on media containing ethidium bromide, an agent that induces loss of mitochondrial DNA and defects in the cell wall (33–35). Notably, *gep4Δ* cells also exhibit growth deficiency under these stress conditions (Fig. 3*A*) (24). If PTPMT1 orthologs function as PGP phosphatases, they should rescue this *GEP4*-knock-out phenotype. Indeed, expression of WT PTPMT1 orthologs effectively restored normal growth, whereas expression of their catalytically inactive CS mutants failed to complement the loss of GEP4 (Fig. 3*A*). Our results indicate that PTPMT1 orthologs from both *Drosophila* and bacteria serve as functional equivalents of GEP4 in yeast.

To examine the steady-state levels of PGP and CL in yeast, total lipids were extracted from [^{32}P]orthophosphate labeled cells and separated by TLC. As previously reported, a detectable amount of PGP has been observed in *gep4Δ* cells, while it was barely measurable in wild type cells (Fig. 3*B*) (24). To further quantify changes in CL levels, we measured the percentage of radioactivity incorporated into phospholipids and subsequently determined the ratio of ^{32}P in PGP *versus* total phospholipids. Loss of GEP4 led to a significant accumulation of PGP, from 0.48% in wild type cells to 2% in *gep4Δ* cells (Fig. 3*D*, *top panel*). More importantly, the individual complementation of mouse, fly, or bacterial PTPMT1 in *gep4Δ* cells alleviated the accumulation of PGP (Fig. 3*B* and *top panel* of Fig. 3D). In contrast, the CS mutant of *R. baltica* PTPMT1 was unable to lower PGP levels (Fig. 3, *B* and *D*), consistent with their *in vitro* PGP phosphatase activities. Furthermore, the expression of PTPMT1 orthologs restored the CL deficiency in *gep4Δ* cells (Fig. 3*C* and *lower panel* of Fig. 3*D*). Conversely, the CS mutant of *R. baltica* PTPMT1 failed to rescue the defect. Taken together, these results indicate that the bacterial and fly PTPMT1 possess PGP phosphatase activity *in vivo* and are crucially involved in maintaining CL level.

The Rhodopirellula PTPMT1 Localizes to the Mitochondrion of Eukaryotes—To compensate for the loss of GEP4 in yeast, bacterial PTPMT1 had to be correctly localized to the mitochondria to access its substrate, PGP. The proper targeting of newly synthesized proteins to the mitochondria is often mediated by a mitochondrial targeting sequence (MTS) comprised of 20–80 amino acids located at the N terminus of the protein (36). Although these peptide signals do not have a conserved primary sequence, they are generally enriched with the positively charged amino acid arginine, have a high percentage of leucine and serine, and contain few if any acidic residues (37, 38). The spacing between the residues often allows the formation of an amphiphilic α-helix, with positively charged and hydrophobic residues on the opposite faces. It has been shown that the first 37 amino acids of *M. musculus* PTPMT1 encompass a MTS (8). When fused to a Green Fluorescent Protein (GFP), these 37 amino acids direct the fluorescent signal exclusively to the mitochondrion. Therefore, we compared the N-terminal regions of *D. melanogaster,* and *R. baltica* PTPMT1 orthologs to that of the mouse protein (Fig. 4*A*). Notably, many basic and hydrophobic residues are conserved among PTPMT1 orthologs. We next plotted the amino acids comprising the regions potentially forming amphiphilic helices onto a helical wheel (Fig. 4*B*). In both *M. musculus* and *R. baltica* PTPMT1, the positive charges grouped on one side, and the hydrophobic residues clustered on the other, thus fitting the MTS model described above.

To determine whether the *Rhodopirellula* PTPMT1 resides in the mitochondria in an *in vivo* setting, we cultured *gep4Δ* yeast cells that were complemented with PTPMT1 orthologs and performed subcellular fractionation. As shown in Fig. 4*C*, both the *R. baltica* and *Drosophila* PTPMT1s are highly enriched in the histodenz gradient-purified mitochondria. The purity of each fraction was further validated by the presence of the mitochondrial marker Porin, the endoplasmic reticulum (ER) marker Calreticulin, as well as the cytoplasma marker Phosphoglycerate Kinase 1/Pgk1. The localization of a bacterial protein to the yeast mitochondria likely indicates the conserva-

FIGURE 2. **Analysis of bacterial PTPMT1 activity *in vitro*.** *A*, specific activities of recombinant murine (*M. mus*), fly (*D. mel*), and bacterial (*R. balt*) PTPMT1 are measured using pNPP as substrate. Data were calculated from the change in absorbance at 410 nm and represented as the mean ± S.D. of triplicate measurements. *CS*, catalytically inactive mutant. *B*, synthesis of ^{14}C-PGP. Highlighted in *blue* is the phosphate group cleaved by PTPMT1 and marked with *red asterisks* are the radiolabled carbons. *C*, activities of wild-type and catalytically inactive PTPMT1 orthologs against PGP. Lipid products from the reactions were separated by TLC and analyzed by autoradiography. A trace amount of PGP phosphatase activity is seen in the background, because a contaminant *E. coli* PGP phosphatase co-purified with the recombinant PGS proteins (18). *D*, phosphatase assay conditions are determined for each indicated enzyme by measuring the amount of free phosphate released using the malachite green reagent. The reaction was carried out at 30 °C and in the presence of 100 μM PGP. Enzyme concentrations are indicated in the *insets. E*, comparison of enzymatic activities. Phosphatase activity was calculated under initial linear rate conditions (30 °C, 100 μM PGP, and 30 s of incubation time), compared with that of *M. mus* PTPMT1, and represented as the mean ± S.D. from three independent experiments. *F*, saturation curve of the *Rhodopirellula* PTPMT1 ortholog. The phosphatase assay was carried out under initial linear rate conditions and in the presence of various PGP concentrations. A nonlinear regression analysis was performed to indicate the saturation. *G*, effect of Triton X-100 on *Rhodopirellula* PTPMT1 PGP phosphatase activity.
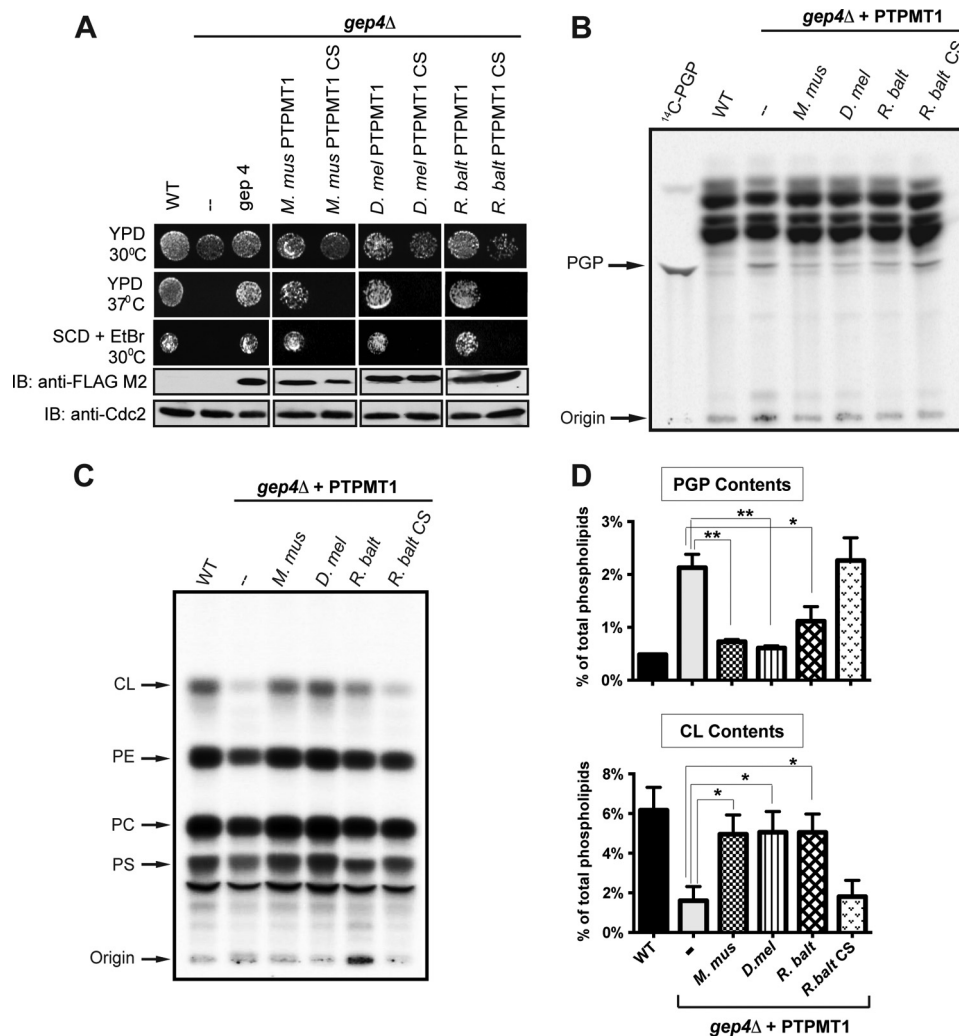
FIGURE 3. **Bacterial PTPMT1 functionally compensates for loss of yeast gep4 *in vivo*.** *A*, wild-type murine, fly, and bacterial PTPMT1 complement the growth deficiency of *GEP4*-null cells. The expression levels of FLAG-tagged PTPMT1s and GEP4 are indicated by Western blot analysis. *YPD*, yeast extract-peptone-glucose medium; *SCD*, synthetic completed medium with dextrose; *EtBr*, ethidium bromide. CDC2 levels are shown as the loading control. Detection of steady state PGP (*B*) and CL (*C*) levels in *gep4Δ* yeast cells complemented with control plasmid or plasmids encoding PTPMT1 orthologs. Cells were labeled with [^{32}P]orthophosphate at 10μCi/ml for 12 h. Lipids were extracted, separated via TLC, and viewed by autoradiography. *D*, PGP and CL contents are determined by the ratio of ^{32}P incorporated into PGP *versus* total phospholipids, and represented as the mean ± S.D. from three independent experiments. **, $p \leq 0.01$; *, $p \leq 0.05$.

tion of the MTS and is consistent with the bacterial origin of mitochondria. We then postulated that this MTS would behave similarly in mammalian cells. To test our hypothesis, a C-terminal GFP-tagged bacterial PTPMT1 was introduced into primate COS-1 cells. Mitochondria were subsequently labeled with MitoTracker Red and the cells were fixed for immunofluorescence analysis. A substantial amount of the *R. baltica* PTPMT1 targeted to the mitochondria as indicated by the co-localization of the two fluorescent signals (Fig. 4*D*). Together, our results suggest that the *R. baltica* PTPMT1 contains a conserved MTS-like sequence, even though *R. baltica* does not have mitochondria. It is not known whether *R. baltica* has any CL-enriched lipid domain, particularly in its internal membrane structures.

DISCUSSION

Raetz *et al.* previously identified three distinct bacterial PGP phosphatases, pgpA, pgpB, and pgpC in *E. coli*, which do not

share any significant domain structure and sequence homology with PTPMT1 (Fig. 1*D*) (39 – 41). A pgpA, pgpB, or pgpC-like phosphatase was not found in *R. baltica* (Fig. 1*E*). The yeast PGP phosphatase GEP4 belongs to the larger haloacid dehalogenase (HAD)-like family and contains a conserved DXDX(T/V) motif in the active site (Fig. 1*D*) (24, 42). Orthologs of GEP4 exist in fungi and plants, as well as several protists, but not in bacteria (9, 24). Our analysis revealed that the prokaryotic *R. baltica* utilizes a PTPMT1-like PGP phosphatase, as opposed to using those existent in yeast (GEP4) or *E. coli* (pgpA, pgpB, and pgpC) to dephosphorylate PGP, suggesting an important role of this phosphatase in *Rhodopirellula*.

R. baltica is a marine bacterium whose genome is first sequenced in 2003 (43). Cultivable stains have not been isolated until recently (44). As such, the phospholipid composition and CL abundance in this organism are presently unknown. Interestingly, our bioinformatics search of *Rhodopirellula* genome identified orthologs of PGP synthase (PGS) and CL synthase
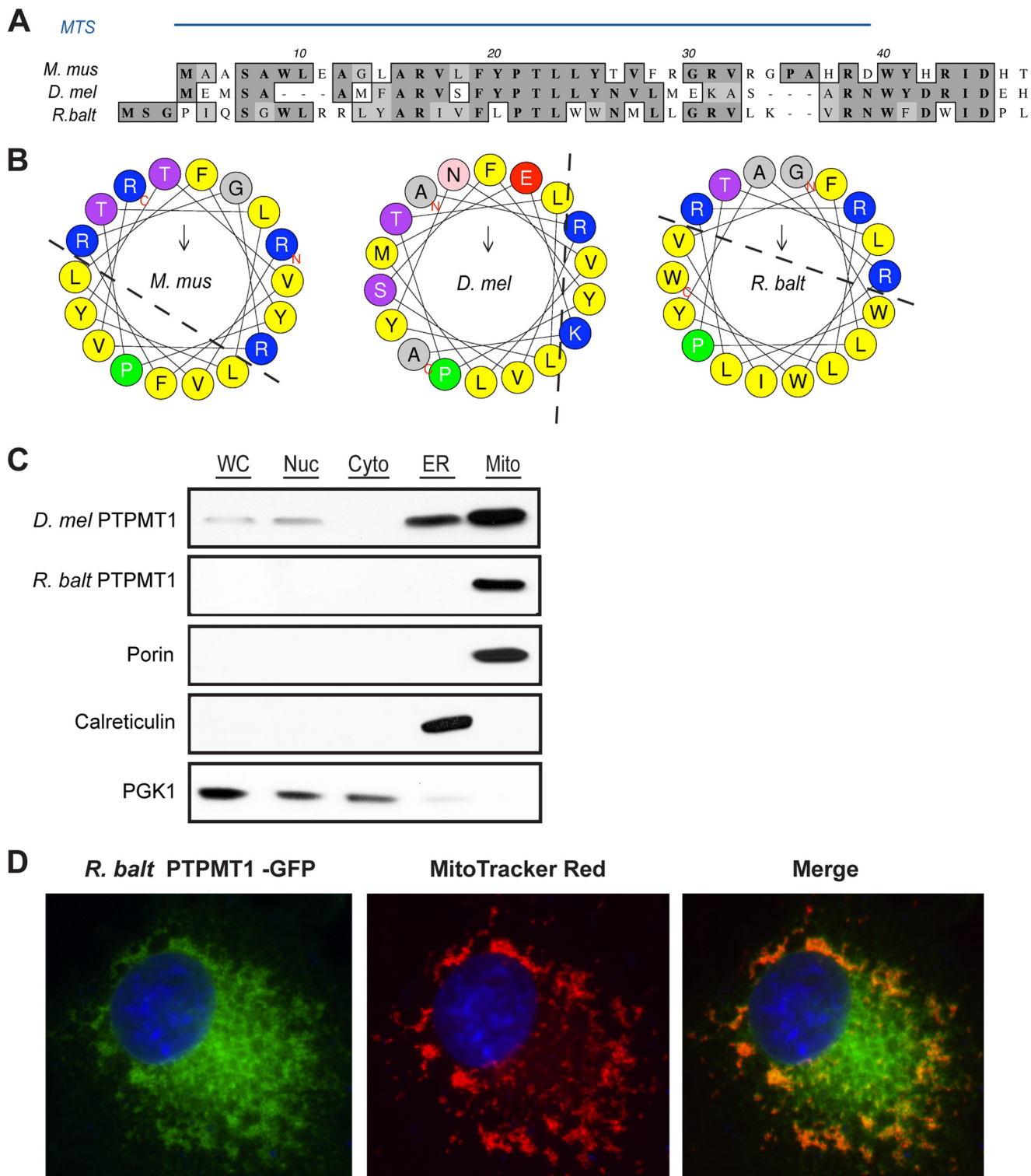
FIGURE 4. **Mitochondrial localization of the *Rhodopirellula* PTPMT1.** *A*, N-terminal sequences of PTPMT1 orthologs are aligned using PROMALS3D. Amino acid similarities are shaded in *light gray* and identities in *dark gray*. The MTS of mouse PTPMT1 has been previously characterized (8) and is indicated by the *blue bar*. *B*, N-terminal region of bacterial PTPMT1 forms an amphiphilic helix. 18 amino-terminal residues were plotted on the helical wheel using HeliQuest (51). Basic residues are colored *blue*, and hydrophobic residues are colored *yellow*. *C*, subcellular fractionation of yeast *gep4Δ* cells expressing fly or bacterial PTPMT1. 30 μg of protein from each fraction were analyzed by SDS-PAGE and immunoblotting. Porin, Calreticulin, and PGK1 serve as marker proteins for mitochondria, ER, and cytosol, respectively. *D*, bacterial PTPMT1 localizes to the mitochondria of mammalian COS-1 cells. 24 h post-transfection, cells were stained with MitoTracker Red, fixed, and analyzed by immunofluoresence imaging.

(CLS) with confidence (Fig. 1*E*). PGS is the first enzyme of CL *de novo* synthesis which facilitates the nucleophilic attack of a glycerol-3-phosphate (G3P) on CDP-diacylglycerol (CDP-

DAG) to generate PGP (Fig. 1*A*) (10). Following the action of PGP phosphatase, CLS converts PG into CL. The presence of all three enzymes of CL *de novo* synthesis in *Rhodopirellula*

genome likely indicates active CL biosynthesis in this organism. To date, genetic manipulation of *Rhodopirellula* genome has not been achieved. Using a yeast mutant strain lacking the PGP phosphatase GEP4, we demonstrated that *R. baltica* PTPMT1 complemented the loss of GEP4, and the rescue is dependent on its phosphatase activity (Fig. 3*A*), suggesting that *Rhodopirellula* PTPMT1 is a functional PGP phosphatase *in vivo*.

R. baltica belongs to the bacterial phylum *Planctomycetes*. Like other plantomycetes, it possesses distinctive features that are uncommon among bacteria, such as peptidoglycan-less cell wall, complex internal structures, and partial compartmentalization. It also encodes endocytosis-like protein uptake and membrane coat-like proteins (27, 28). The unique eukaryote-like features of planctomycetes challenge the current hypothesis regarding the origin of eukaryotic organelles (27). Because of their complex endomembrane system, *Planctomycetes* together with *Verrucomicrobia* and *Chlamydiae* form the PVC superphylum in eubacteria and are thought to represent the intermediates of prokaryote and eukaryote evolution (29). Notably, PTPMT1-like sequences were also found in two species of *Chlamydiae*, *Simkania negevensis* and *Candidatus Protochlamydia amoebophila*. Our results suggested that *Rhodopirellula* contains a unique mammalian-type PGP phosphatase that could potentially play an important role in the organism CL metabolism.

Ectopically expressed *R. baltica* PTPMT1 was localized to the mitochondria of yeast and mammalian cells (Fig. 4, *C* and *D*), suggesting the existence of a conserved region that could function as a MTS in eukaryotes. In mammals, the mitochondrial proteome contains over 1000 proteins, of which the majority are encoded in the nucleus and subsequently transported into the mitochondria (45). Many imported proteins have a characteristic MTS composed of amphiphilic α-helix forming amino acids and recognized by the Translocase of the Outer Membrane (TOM) and Translocase of the Inner Membrane (TIM) complexes of mitochondria (46). Our sequence alignment and helical wheel analysis revealed that the N terminus of *R. baltica* PTPMT1 contains several conserved positively charged and hydrophobic amino acids, which would form an amphiphilic helix (Fig. 4*A*). Interestingly, a number of bacterial proteins have been shown to contain functional MTS when expressed in mammalian cells, including the enteropathogenic *E. coli* effectors EspF and Map (47). The existence of MTS in bacterial proteins may reflect an evolutionarily conserved mechanism for selective protein transport and domain organization.

In summary, we have identified a mammalian-type PGP phosphatase in the bacterium *R. baltica*. We performed biochemical and gene complementation assays to subsequently validate our initial bioinformatic search. The ability of the bacterial phosphatase to target to eukaryotic mitochondria suggests the existence of a conserved mitochondrial targeting sequence despite the absence of mitochondrion in bacteria. The *R. baltica* PTPMT1 may function at the organization center for enzymes involved in the biosynthesis of CL in this organism.

REFERENCES

1. Hunter, T. (1987) A thousand and one protein kinases. *Cell* **50,** 823–829
2. Alonso, A., Sasin, J., Bottini, N., Friedberg, I., Osterman, A., Godzik, A., Hunter, T., Dixon, J., and Mustelin, T. (2004) Protein tyrosine phosphatases in the human genome. *Cell* **117,** 699–711
3. Tonks, N. K., and Neel, B. G. (2001) Combinatorial control of the specificity of protein tyrosine phosphatases. *Curr. Opin. Cell Biol.* **13,** 182–195
4. Fauman, E. B., and Saper, M. A. (1996) Structure and function of the protein tyrosine phosphatases. *Trends Biochem. Sci* **21,** 413–417
5. Tagliabracci, V. S., Turnbull, J., Wang, W., Girard, J. M., Zhao, X., Skurat, A. V., Delgado-Escueta, A. V., Minassian, B. A., Depaoli-Roach, A. A., and Roach, P. J. (2007) Laforin is a glycogen phosphatase, deficiency of which leads to elevated phosphorylation of glycogen *in vivo. Proc. Natl. Acad. Sci. U.S.A.* **104,** 19262–19266
6. Worby, C. A., Gentry, M. S., and Dixon, J. E. (2006) Laforin, a dual specificity phosphatase that dephosphorylates complex carbohydrates. *J. Biol. Chem.* **281,** 30412–30418
7. Maehama, T., and Dixon, J. E. (1998) The tumor suppressor, PTEN/MMAC1, dephosphorylates the lipid second messenger, phosphatidylinositol 3,4,5-trisphosphate. *J. Biol. Chem.* **273,** 13375–13378
8. Pagliarini, D. J., Wiley, S. E., Kimple, M. E., Dixon, J. R., Kelly, P., Worby, C. A., Casey, P. J., and Dixon, J. E. (2005) Involvement of a mitochondrial phosphatase in the regulation of ATP production and insulin secretion in pancreatic beta cells. *Mol Cell* **19,** 197–207
9. Zhang, J., Guan, Z., Murphy, A. N., Wiley, S. E., Perkins, G. A., Worby, C. A., Engel, J. L., Heacock, P., Nguyen, O. K., Wang, J. H., Raetz, C. R., Dowhan, W., and Dixon, J. E. (2011) Mitochondrial phosphatase PTPMT1 is essential for cardiolipin biosynthesis. *Cell Metab* **13,** 690–700
10. Schlame, M. (2008) Cardiolipin synthesis for the assembly of bacterial and mitochondrial membranes. *J. Lipid Res.* **49,** 1607–1620
11. Cronan, J. E. (2003) Bacterial membrane lipids: where do we stand? *Annu. Rev. Microbiol.* **57,** 203–224
12. Tan, B. K., Bogdanov, M., Zhao, J., Dowhan, W., Raetz, C. R., and Guan, Z. (2012) Discovery of a cardiolipin synthase utilizing phosphatidylethanolamine and phosphatidylglycerol as substrates. *Proc. Natl. Acad. Sci. U.S.A.* **109,** 16504–16509
13. Pei, J., Tang, M., and Grishin, N. V. (2008) PROMALS3D web server for accurate multiple protein sequence and structure alignments. *Nucleic Acids Res.* **36,** W30–34
14. Tamura, K., Peterson, D., Peterson, N., Stecher, G., Nei, M., and Kumar, S. (2011) MEGA5: molecular evolutionary genetics analysis using maximum likelihood, evolutionary distance, and maximum parsimony methods. *Mol Biol Evol* **28,** 2731–2739
15. Punta, M., Coggill, P. C., Eberhardt, R. Y., Mistry, J., Tate, J., Boursnell, C., Pang, N., Forslund, K., Ceric, G., Clements, J., Heger, A., Holm, L., Sonnhammer, E. L., Eddy, S. R., Bateman, A., and Finn, R. D. (2012) The Pfam protein families database. *Nucleic Acids Res.* **40,** D290–301
16. Marchler-Bauer, A., Anderson, J. B., Cherukuri, P. F., DeWeese-Scott, C., Geer, L. Y., Gwadz, M., He, S., Hurwitz, D. I., Jackson, J. D., Ke, Z., Lanczycki, C. J., Liebert, C. A., Liu, C., Lu, F., Marchler, G. H., Mullokandov, M., Shoemaker, B. A., Simonyan, V., Song, J. S., Thiessen, P. A., Yamashita, R. A., Yin, J. J., Zhang, D., and Bryant, S. H. (2005) CDD: a Conserved Domain Database for protein classification. *Nucleic Acids Res.* **33,** D192–196
17. de Castro, E., Sigrist, C. J., Gattiker, A., Bulliard, V., Langendijk-Genevaux, P. S., Gasteiger, E., Bairoch, A., and Hulo, N. (2006) ScanProsite: detection of PROSITE signature matches and ProRule-associated functional and structural residues in proteins. *Nucleic Acids Res.* **34,** W362–365
18. Xiao, J., Engel, J. L., Zhang, J., Chen, M. J., Manning, G., and Dixon, J. E. (2011) Structural and functional analysis of PTPMT1, a phosphatase required for cardiolipin synthesis. *Proc. Natl. Acad. Sci. U.S.A.* **108,** 11860–11865
19. Taylor, G. S., Maehama, T., and Dixon, J. E. (2000) Myotubularin, a protein tyrosine phosphatase mutated in myotubular myopathy, dephosphorylates the lipid second messenger, phosphatidylinositol 3-phosphate. *Proc. Natl. Acad. Sci. U.S.A.* **97,** 8910–8915
20. Dowhan, W. (1992) Phosphatidylglycerophosphate synthase from *Esche-*

richia coli. Methods Enzymol. **209,** 313–321

21. Maehama, T., Taylor, G. S., Slama, J. T., and Dixon, J. E. (2000) A sensitive assay for phosphoinoside phosphatases. *Anal. Biochem.* **279,** 248–250

22. Brachmann, C. B., Davies, A., Cost, G. J., Caputo, E., Li, J., Hieter, P., and Boeke, J. D. (1998) Designer deletion strains derived from *Saccharomyces cerevisiae* S288C: a useful set of strains and plasmids for PCR-mediated gene disruption and other applications. *Yeast* **14,** 115–132

23. Chang, S. C., Heacock, P. N., Clancey, C. J., and Dowhan, W. (1998) The PEL1 gene (renamed PGS1) encodes the phosphatidylglycero-phosphate synthase of *Saccharomyces cerevisiae. J. Biol. Chem.* **273,** 9829–9836

24. Osman, C., Haag, M., Wieland, F. T., Brugger, B., and Langer, T. (2010) A mitochondrial phosphatase required for cardiolipin biosynthesis: the PGP phosphatase Gep4. *EMBO J.* **29,** 1976–1987

25. Glick, B. S., and Pon, L. A. (1995) Isolation of highly purified mitochondria from *Saccharomyces cerevisiae. Methods Enzymol.* **260,** 213–223

26. Pagliarini, D. J., Worby, C. A., and Dixon, J. E. (2004) A PTEN-like phosphatase with a novel substrate specificity. *J. Biol. Chem.* **279,** 38590–38596

27. Fuerst, J. A., and Sagulenko, E. (2011) Beyond the bacterium: planctomycetes challenge our concepts of microbial structure and function. *Nat. Rev. Microbiol.* **9,** 403–413

28. Lindsay, M. R., Webb, R. I., Strous, M., Jetten, M. S., Butler, M. K., Forde, R. J., and Fuerst, J. A. (2001) Cell compartmentalisation in planctomycetes: novel types of structural organisation for the bacterial cell. *Arch. Microbiol.* **175,** 413–429

29. Devos, D. P., and Reynaud, E. G. Evolution. (2010) Intermediate steps. *Science* **330,** 1187–1188

30. Pearson, G., Robinson, F., Beers Gibson, T., Xu, B. E., Karandikar, M., Berman, K., and Cobb, M. H. (2001) Mitogen-activated protein (MAP) kinase pathways: regulation and physiological functions. *Endocr. Rev.* **22,** 153–183

31. Chang, Y. Y., and Kennedy, E. P. (1967) Phosphatidyl glycerophosphate phosphatase. *J. Lipid Res.* **8,** 456–462

32. Kelly, B. L., and Greenberg, M. L. (1990) Characterization and regulation of phosphatidylglycerolphosphate phosphatase in *Saccharomyces cerevisiae. Biochim. Biophys. Acta* **1046,** 144–150

33. Janitor, M., and Subik, J. (1993) Molecular cloning of the PEL1 gene of *Saccharomyces cerevisiae* that is essential for the viability of petite mutants. *Curr Genet* **24,** 307–312

34. Jiang, F., Ryan, M. T., Schlame, M., Zhao, M., Gu, Z., Klingenberg, M., Pfanner, N., and Greenberg, M. L. (2000) Absence of cardiolipin in the crd1 null mutant results in decreased mitochondrial membrane potential and reduced mitochondrial function. *J. Biol. Chem.* **275,** 22387–22394

35. Pfeiffer, K., Gohil, V., Stuart, R. A., Hunte, C., Brandt, U., Greenberg, M. L., and Schägger, H. (2003) Cardiolipin stabilizes respiratory chain super-complexes. *J. Biol. Chem.* **278,** 52873–52880

36. Omura, T. (1998) Mitochondria-targeting sequence, a multi-role sorting sequence recognized at all steps of protein import into mitochondria. *J. Biochem.* **123,** 1010–1016

37. Roise, D., Horvath, S. J., Tomich, J. M., Richards, J. H., and Schatz, G.

(1986) A chemically synthesized pre-sequence of an imported mitochondrial protein can form an amphiphilic helix and perturb natural and artificial phospholipid bilayers. *EMBO J.* **5,** 1327–1334

38. von Heijne, G. (1986) Mitochondrial targeting sequences may form amphiphilic helices. *EMBO J.* **5,** 1335–1342

39. Icho, T., and Raetz, C. R. (1983) Multiple genes for membrane-bound phosphatases in *Escherichia coli* and their action on phospholipid precursors. *J. Bacteriol.* **153,** 722–730

40. Funk, C. R., Zimniak, L., and Dowhan, W. (1992) The pgpA and pgpB genes of *Escherichia coli* are not essential: evidence for a third phosphatidylglycerophosphate phosphatase. *J. Bacteriol.* **174,** 205–213

41. Lu, Y. H., Guan, Z., Zhao, J., and Raetz, C. R. (2011) Three phosphatidyl-glycerol-phosphate phosphatases in the inner membrane of *Escherichia coli. J. Biol. Chem.* **286,** 5506–5518

42. Collet, J. F., Stroobant, V., Pirard, M., Delpierre, G., and Van Schaftingen, E. (1998) A new class of phosphotransferases phosphorylated on an aspartate residue in an amino-terminal DXDX(T/V) motif. *J. Biol. Chem.* **273,** 14107–14112

43. Glöckner, F. O., Kube, M., Bauer, M., Teeling, H., Lombardot, T., Ludwig, W., Gade, D., Beck, A., Borzym, K., Heitmann, K., Rabus, R., Schlesner, H., Amann, R., and Reinhardt, R. (2003) Complete genome sequence of the marine planctomycete Pirellula sp. strain 1. *Proc. Natl. Acad. Sci. U.S.A.* **100,** 8298–8303

44. Winkelmann, N., and Harder, J. (2009) An improved isolation method for attached-living Planctomycetes of the genus Rhodopirellula. *J. Microbiol. Methods* **77,** 276–284

45. Pagliarini, D. J., Calvo, S. E., Chang, B., Sheth, S. A., Vafai, S. B., Ong, S. E., Walford, G. A., Sugiana, C., Boneh, A., Chen, W. K., Hill, D. E., Vidal, M., Evans, J. G., Thorburn, D. R., Carr, S. A., and Mootha, V. K. (2008) A mitochondrial protein compendium elucidates complex I disease biology. *Cell* **134,** 112–123

46. Habib, S. J., Neupert, W., and Rapaport, D. (2007) Analysis and prediction of mitochondrial targeting signals. *Methods Cell Biol.* **80,** 761–781

47. Papatheodorou, P., Domańska, G., Oxle, M., Mathieu, J., Selchow, O., Kenny, B., and Rassow, J. (2006) The enteropathogenic *Escherichia coli* (EPEC) Map effector is imported into the mitochondrial matrix by the TOM/Hsp70 system and alters organelle morphology. *Cell Microbiol.* **8,** 677–689

48. Corcelli, A. (2009) The cardiolipin analogues of Archaea. *Biochim. Biophys. Acta* **1788,** 2101–2106

49. Pei, J., Kim, B. H., and Grishin, N. V. (2008) PROMALS3D: a tool for multiple protein sequence and structure alignments. *Nucleic Acids Res.* **36,** 2295–2300

50. Gouet, P., Courcelle, E., Stuart, D. I., and Métoz, F. (1999) ESPript: analysis of multiple sequence alignments in PostScript. *Bioinformatics* **15,** 305–308

51. Gautier, R., Douguet, D., Antonny, B., and Drin, G. (2008) HELIQUEST: a web server to screen sequences with specific α-helical properties. *Bioinformatics* **24,** 2101–2102